

Received: 2021.07.12

Accepted: 2021.09.10

Available online: 2021.09.25

Published: 2021.10.26

Platypnea Orthodeoxia Due to a Patent Foramen Ovale and Intrapulmonary Shunting After Severe COVID-19 Pneumonia

Authors' Contribution:

Study Design A
Data Collection B
Statistical Analysis C
Data Interpretation D
Manuscript Preparation E
Literature Search F
Funds Collection G

EF 1 **Blair K. Dodson**
EF 2 **C. Kendall Major**
EF 1 **Maxwell Grant**
E 1 **Byung Soo Yoo** 
E 1 **B. Mitchell Goodman**

1 Department of Internal Medicine, Eastern Virginia Medical School, Norfolk, VA, USA

2 Department of Medicine, Hospital of the University of Pennsylvania, Philadelphia, PA, USA

Corresponding Author: Blair K. Dodson, e-mail: dodsonbk@evms.edu
Financial support: None declared
Conflict of interest: None declared

Patient: **Male, 85-year-old**
Final Diagnosis: **Platypnea orthodeoxia**
Symptoms: **Dyspnea • orthostatic intolerance**
Medication: —
Clinical Procedure: —
Specialty: **Infectious Diseases**

Objective: **Unusual clinical course**

Background: Platypnea orthodeoxia syndrome (POS) presents with positional dyspnea and hypoxemia defined as arterial desaturation of at least 5% or a drop in PaO₂ of at least 4 mmHg. Causes of POS include a variety of cardiopulmonary etiologies and has been reported in patients recovering from severe COVID-19 pneumonia. However, clinical presentation and outcomes in a patient with multiple interrelated mechanisms of shunting has not been documented.

Case Report: An 85-year-old man hospitalized for hypertensive emergency and severe COVID-19 pneumonia was diagnosed with platypnea orthodeoxia on day 28 of illness. During his disease course, the patient required supplemental oxygen by high-flow nasal cannula but never required invasive mechanical ventilation. Chest imaging revealed evolving mixed consolidation and ground-glass opacities with a patchy and diffuse distribution, involving most of the left lung. Echocardiography was ordered to evaluate for intracardiac shunt, which revealed a patent foramen ovale. Closure of the patent foramen ovale was not pursued. Management included graded progression to standing and supplemental oxygen increases when upright. The patient was discharged to a skilled nursing facility and his positional oxygen requirement resolved on approximately day 78.

Conclusions: The present case highlights the multiple interrelated mechanisms of shunting in patients with COVID-related lung disease and a patent foramen ovale. Eight prior cases of POS after COVID-19 pneumonia have been reported to date but none with a known patent foramen ovale. In patients with persistent positional oxygen requirements at follow-up, quantifying shunt fraction over time through multiple modalities can guide treatment decisions.

Keywords: **Case Reports • COVID-19 • Foramen Ovale, Patent**

Full-text PDF: <https://www.amjcaserep.com/abstract/index/idArt/933975>



2080



4



31



Background

Platypnea orthodeoxia syndrome (POS) is the clinical phenomenon of acquired right-to-left shunt, resulting in dyspnea and hypoxemia in the upright position [1,2]. Hypoxemia in this setting is defined as a drop in partial pressure of oxygen (PaO_2) by 4 mmHg or oxygen saturation (SaO_2) by 5%. In order to meet diagnostic criteria, both symptoms must quickly improve once the patient is returned to a recumbent position [1]. Causes of POS include a variety of cardiopulmonary etiologies [1-6].

Recent reports have documented the development of POS in patients who are recovering from severe COVID-19 infection [7-9]. The underlying mechanism of lung damage in COVID-19 patients is complex. To date, there are no known pathognomonic characteristics. Over the course of the pandemic, the prevailing theory has evolved from a picture of “typical” acute respiratory distress syndrome (ARDS) and fibrotic evolution to more recent reviews describing a comparative prominence of airway and pleural inflammation, small-to-medium-sized artery thrombosis, vasculitis, and endotheliitis [10-24]. Whether diffuse alveolar damage in COVID-19 differs from other etiologies causing ARDS has not been determined [11].

The primary mechanism of COVID-19-associated POS is considered to be ventilation/perfusion (V/Q) mismatch. Patients with lung damage in the bases are rendered more sensitive to the physiologic increase in V/Q mismatch that occurs with standing [1,7,25]. Microangiopathy and thromboembolism may also contribute to V/Q mismatching [7]. Prior publications have not reported on the role that intracardiac shunting may play in the development of POS in COVID-19 patients [7,25]. However, Dessap et al described the clinical significance of intracardiac shunts in ARDS [26]. Up to one-fifth of patients with ARDS were deemed to have a portion of their recalcitrant hypoxemia attributed to an intracardiac shunt. In this report, we investigated the case of a patient who developed POS while recovering from COVID-19 infection. In addition to the extracardiac shunting from interstitial lung disease, the patient was found to have intracardiac shunting related to a patent foramen ovale (PFO) and an associated atrial septal aneurysm. The present case is the first reported case of intracardiac and extracardiac shunting causing platypnea orthodeoxia after COVID-19 pneumonia.

Case Report

An 85-year-old man (BMI 21.24 kg/m^2) with a past medical history of hypothyroidism, hyperlipidemia, and type 2 diabetes mellitus presented to the Emergency Department after a fall and was found to be in hypertensive emergency with a left temporal lobe hemorrhage. The patient was febrile to

38.4°C, slightly tachycardic at 101 beats per minute, and hypertensive at 186/94 mmHg. At that time, the patient had no subjective symptoms of respiratory distress but was found to be hypoxic with an oxygen saturation of 91% on ambient air. He received oxygen supplementation by nasal cannula (NC), with improvement in his oxygen saturation. The initial physical exam was unrevealing. Laboratory analyses were notable for elevations in CPK (359 U/L), troponin (34 ng/L), D-dimer (2.70 mg/L), NT proBNP (649 pg/mL), procalcitonin (0.3 ng/mL), LDH (482 U/L), ferritin (611 ng/mL), fibrinogen (646 mg/dL), and C-reactive protein (11.4 mg/dL). Sodium was low at (130 mmol/L). PT-INR was in normal range (0.98). The initial chest X-ray (CXR) did not reveal any acute or chronic cardiopulmonary abnormalities (Figure 1A). Due to the presence of fever, elevated inflammatory markers, and hypoxia, infection with COVID-19 was suspected and PCR testing was positive for the same. At that time, the patient was started on subcutaneous enoxaparin at therapeutic dose, due to a D-dimer value greater than 2.0, as per institutional protocol. On hospital day 3, the patient began to experience dyspnea associated with desaturations on pulse oximeter as low as 70% on 6 LNC. At that time, he was placed on high-flow nasal cannula (HFNC) at 75% and 45 L, with saturation improvement to >88%. This event prompted a repeat CXR, which revealed interval development of multifocal airspace disease, most likely representing multifocal pneumonia (Figure 1B). At this time, treatment for severe COVID-19 pneumonia commenced per institutional protocols in place at the time and was as follows: Convalescent plasma per institutional protocols, remdesivir 200 mg i.v. once and 100 mg i.v. daily for 4 more days and dexamethasone (6 mg i.v. for 10 days). In the subsequent days, his oxygen requirement slowly decreased, and he was transitioned from HFNC to 5L by NC. He was discharged to a skilled nursing facility (SNF) on 4 L by NC after 15 days of hospitalization, when his condition appeared to plateau in terms of his oxygen requirement and management of his medical co-morbidities.

Two days after discharge to the SNF and approximately day 17 after diagnosis, he re-presented to the Emergency Department after an oxygen desaturation to 77% on 6 L by NC. A physical exam demonstrated bilateral wheezing and rhonchi. He required high-flow oxygen at 60% and 25L to improve his O₂ saturation to 92%. Laboratory studies were notable for elevations in WBC (17.4 K/uL), troponin (32 ng/L), NT proBNP (669 pg/ml), D-dimer (14.40 mg/L), C-reactive protein (12.2 mg/dL), and ferritin (762 ng/ml). All values were elevated compared to the prior admission values. Blood cultures showed no growth. Urinalysis revealed evidence of infection and, in fact, a urine culture showed greater than 100 000 org/ml *Morganella morganii*. CXR demonstrated improvement overall in previously noted multifocal opacities with a similar distribution (Figure 1C). Computed tomography angiography (CTA) did not reveal a pulmonary embolism but demonstrated extensive ground-glass opacities

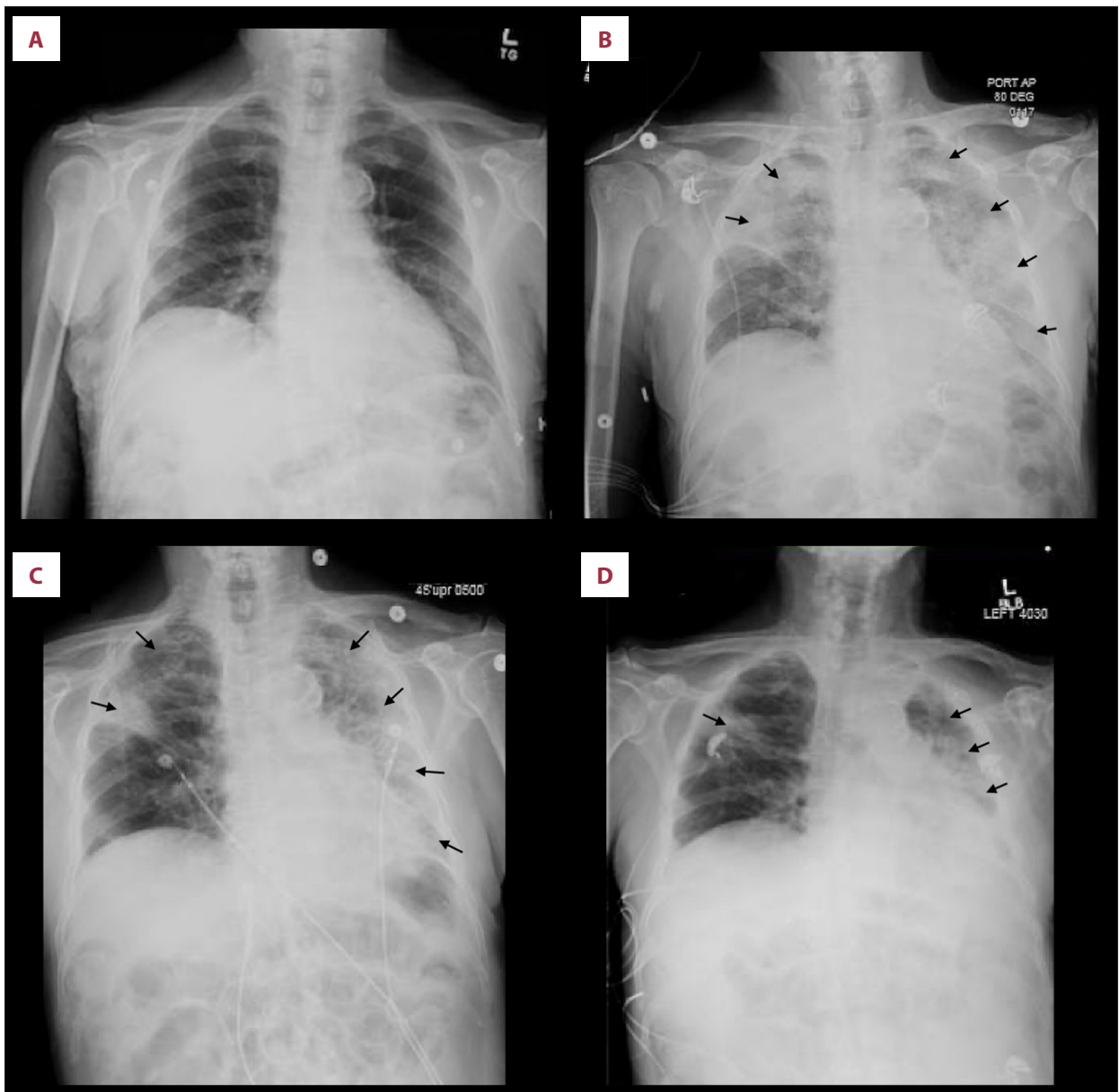


Figure 1. (A) Chest X-ray (CXR) on day 1 of first diagnosis showing no baseline cardiopulmonary abnormalities. (B) CXR on day 3 of illness demonstrating significant multifocal opacities. (C) CXR on day 1 of second hospital admission, day 16 of illness demonstrating interval improvement in right multifocal opacities, evidence of scarring in right upper lobe. (D) CXR showing continued improvement but persistent scarring in right upper lobe (*black arrows*). Figures created using eUnity v7.0.0.1.3. Client Outlook, Inc. Ontario, Canada and macOs Big Sur operating system Version 11.4.

and consolidative processes consistent with COVID-19 pneumonia involving almost the entire left lung, right posterolateral upper lobe, and posterior right lower lobe (**Figure 2**). A transthoracic echocardiogram (TTE) showed an ejection fraction (EF) of 59% without evidence of right heart strain. The patient was admitted and treated for acute hypoxic respiratory failure due to presumed hospital-acquired pneumonia (HAP). Dexamethasone at 6 mg i.v. daily was restarted.

Over the next several days the patient's leukocytosis resolved and inflammatory markers trended down. The patient had a decreasing oxygen requirement at rest. Multiple attempts at the six-minute walk test were undertaken to determine oxygen requirement, with repeated and consistent desaturation to 70% on 5L by NC and orthostatic intolerance. The patient did not experience subjective dyspnea nor did he develop increased work of breathing. A repeat CXR revealed atelectasis, prominent interstitial lung markings, and scarring (**Figure 1D**).

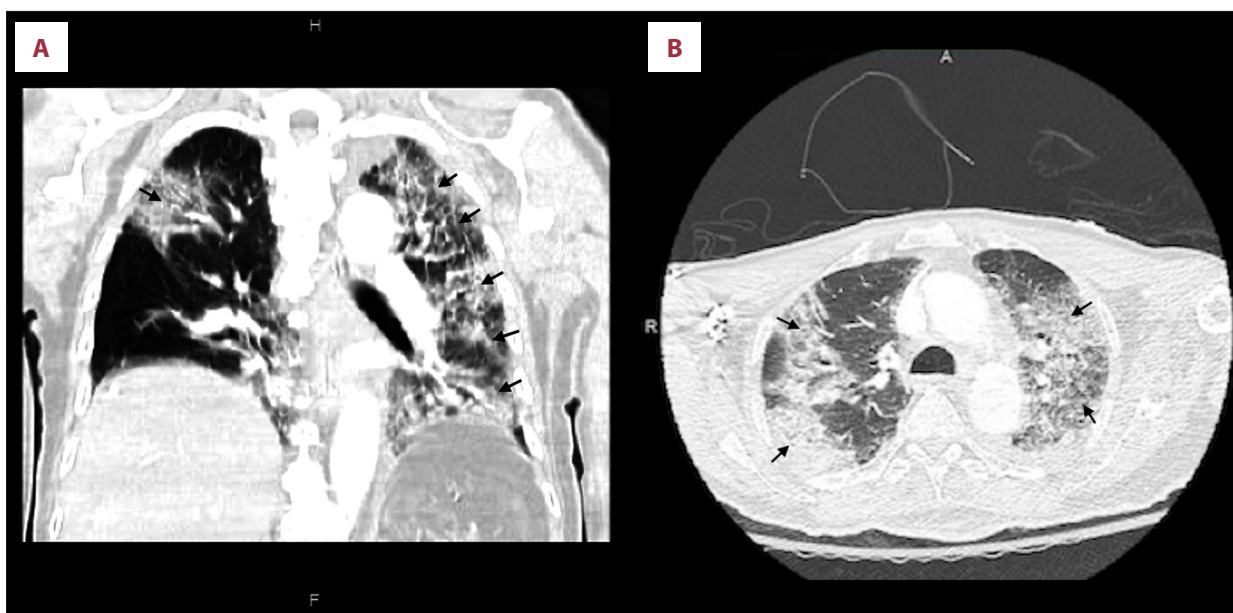


Figure 2. (A) Coronal and (B) axial CT views showing multifocal ground-glass opacities and consolidation involving the entire left lung, right posterolateral upper lobe, and posterior right lower lobe (black arrows). Figures created using eUnity v7.0.0.1.3. Client Outlook, inc, Ontario, Canada and macOs Big Sur operating system Version 11.4.

The patient was diagnosed with platypnea orthodeoxia on day 28 after first diagnosis.

The patient's persistent platypnea orthodeoxia prompted repeat TTE imaging with agitated saline to evaluate for intracardiac shunt, which revealed a PFO and associated atrial septal aneurysm (ASA) (Figure 3). TTE also demonstrated an EF of 75% with near total left ventricular cavity obliteration and an elevated pulmonary artery pressure at 65 mm Hg but normal right ventricular size and function. Empiric closure of the PFO was not pursued during the present admission, favoring a conservative strategy of watchful waiting as the patient is monitored for further recovery from lung changes related to severe COVID-19 infection. He was discharged to a SNF on 4 L by nasal cannula with orders for continued non-pharmacologic interventions such as graded progression to standing and increasing the amount of supplemental oxygen while upright. At first follow-up, approximately 78 days after the first diagnosis, the patient had been discharged home after a short stay in a SNF. He no longer has positional desaturations and no longer requires oxygen at rest. The patient continues to have exertional hypoxemia with desaturations to the mid 80s while ambulating. A repeat TTE was performed, which showed reduction in pulmonary hypertension from 65 mmHg to 37 mmHg pulmonary arterial systolic pressure.

Discussion

Shunts causing POS are characterized as either intracardiac, extracardiac, or miscellaneous (Figure 4) [1,27]. Intracardiac

shunts resulting in POS require both a structural and a functional anomaly. They are further divided into those with normal right atrial pressure (RAP) compared to those with increased RAP (Figure 4) [1,27]. In either setting, blood is shunted through a defect in the atrial septum. Examples of such defects include: patent foramen ovale (PFO), atrial septal defect (Figure 4) [1,27] (ASD), atrial septal aneurysm (ASA) with associated septal defects, and unroofed coronary sinus. Shunts acquired iatrogenically include the Fontan procedure and transcatheter mitral valve repair (Figure 4) [1,27].

Extracardiac shunts are pulmonary shunts and are stratified into true shunts and ventilation and perfusion (V/Q) mismatches (Figure 4) [1,27]. True shunts, also known as intrapulmonary shunts, include pulmonary AVMs, hepatopulmonary syndrome, or large physiologic shunts (Figure 4) [1,27]. Acute respiratory distress syndrome (ARDS) and pleural effusion are examples of physiologic shunts. In contrast, V/Q mismatches occur in lung parenchymal damage as can occur with interstitial lung disease or preferential alveolar filling of the bases in cases of bacterial pneumonia, acute interstitial pneumonia, or organizing pneumonia (Figure 4) [1,27]. These processes occurring in the lung bases result in platypnea orthodeoxia because these patients already have shunting in the bases and upon standing have additional physiologic shunting due to V/Q mismatching in the upper lobes (Figure 4) [1,27]. Patients present with varying degrees of postural desaturation depending on the total shunt fraction (Q_s/Q_t , or the fraction of blood flow that bypasses oxygenation). This point is made evident by the fact that pulmonary vein arterial saturation (CaO_2) is

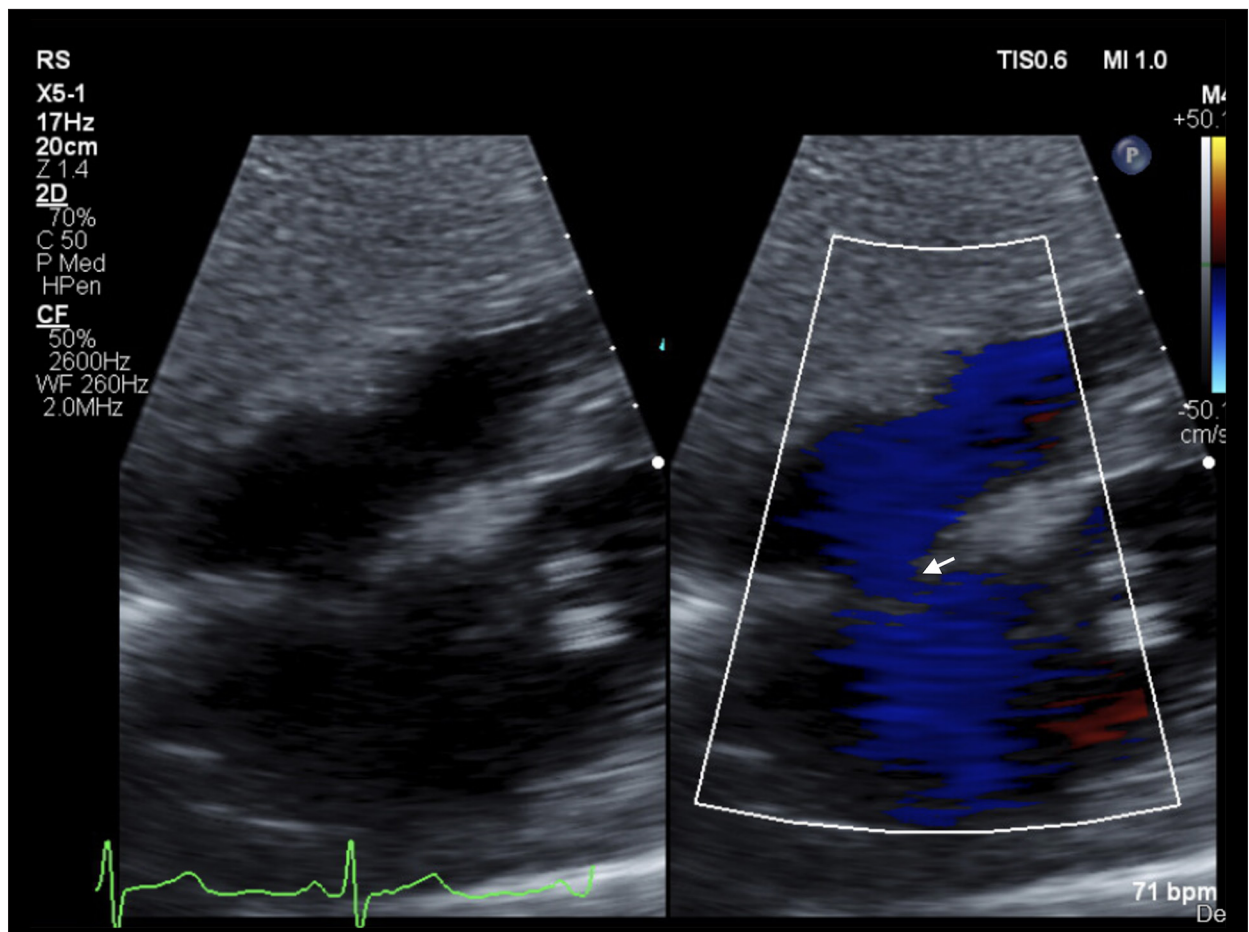


Figure 3. Transthoracic echocardiography, subcostal view, color Doppler showing flow through the atrial septal defect (*white arrow*). Positive bubble study not shown. Figures created using eUnity v7.0.0.1.3. Client outlook Inc. Ontario, Canada and macOS Big Sur operating system Version 11.4.

directly related to the shunt fraction multiplied by the pulmonary artery venous saturation (CvO₂) by the following equation (**Figure 4**) [1,27]:

$$CaO_2 = Q_s/Q_t \times CvO_2 + (1 - Q_s/Q_t) \times CcO_2$$

Severe COVID-19 infections are marked by significant acute and possibly chronic destruction of pulmonary parenchyma [13]. It stands to reason that the incidence of platypnea orthodeoxia exacerbated by extracardiac shunts will parallel the incidence of severe COVID-19 pneumonia. Patients with congenital or acquired intracardiac shunts are at increased risk for additional shunting due to the associated rise in pulmonary artery pressure that accompanies parenchymal lung damage (**Figure 4**) [1]. Micro- and macroangiopathy, which are becoming notable and specific features of COVID-19 pneumonia, may also contribute to V/Q differences. Consequently, these patients may have a clinically relevant increase in the shunt fraction compared to those who do not have an additional pre-existing intracardiac shunt. **Figure 4** summarizes the

mechanisms of shunting and the arrows represent causes of shunt in the present case.

Given these concerns, a diagnostic work-up for the presence of an intracardiac shunt should be considered in post-COVID-19 pneumonia patients experiencing positional desaturations. The initial diagnostic test of choice is TTE with agitated saline bubble study. Images of the right atrium and left atrium should be recorded prior to saline injection and continue for at least 3 cardiac cycles in order to define a shunt as early (intracardiac) or late (pulmonary) [1]. Subcostal views with color Doppler should also be obtained. TTE can be performed in the supine and upright position to estimate the degree of change in shunt fraction [1]. A V/Q scan can estimate the fraction of V/Q mismatching within the lung in the upright and supine positions [1]. V/Q scans can also identify extrapulmonary shunting (ie, the presence of an intracardiac shunt) [1,7,25]. Quantification of extracardiac shunting with V/Q imaging has the potential to factor into which patients are considered for antifibrotic therapy [1,16,25].

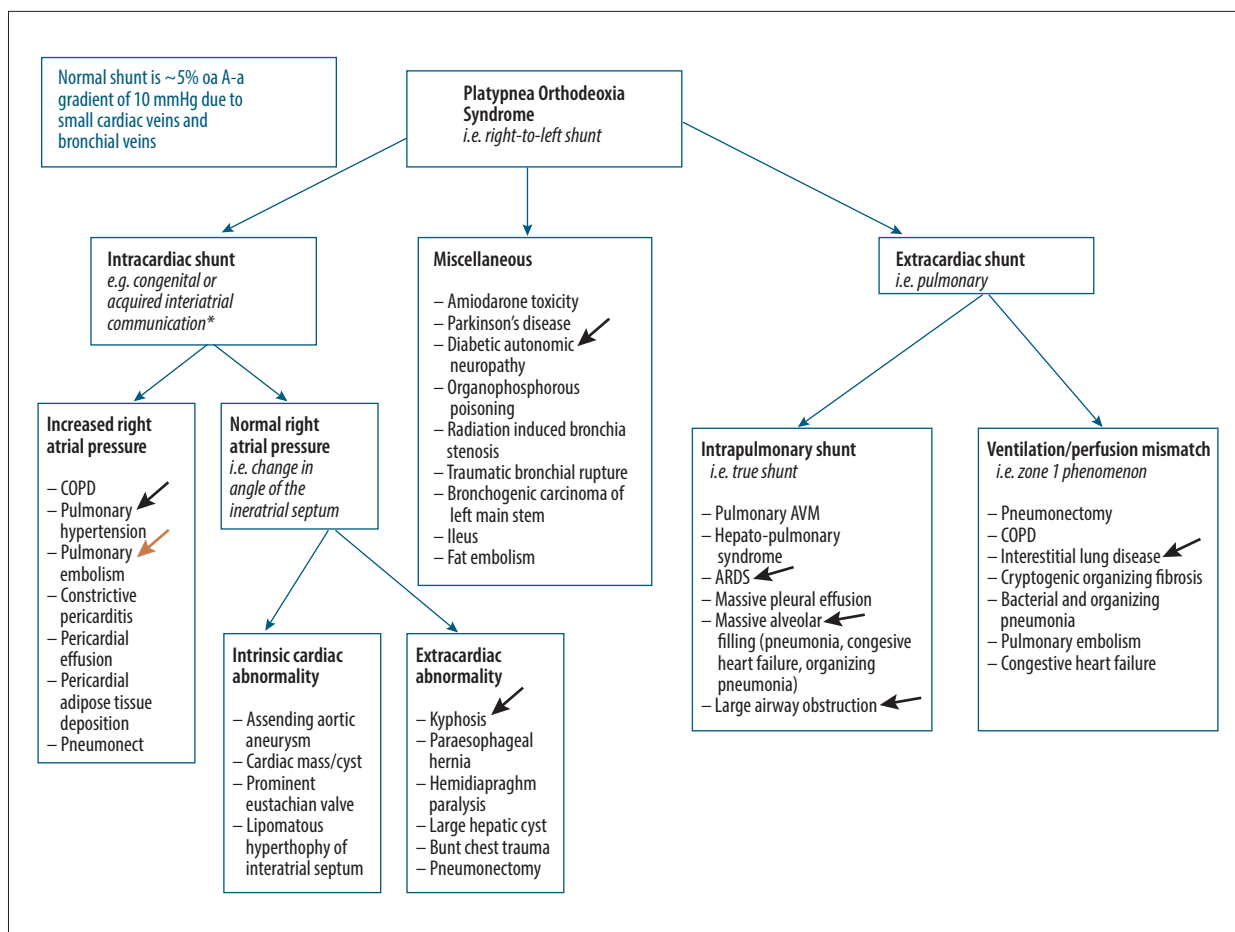


Figure 4. Platypnea orthodeoxia syndrome etiology [1,27]. * Patent foramen ovale, atrial septal defect, atrial septal aneurysm with associated septal defect, partial anomalous pulmonary venous return, unroofed coronary sinus, and other possible mechanisms of shunting. *Black arrows* represent mechanisms of shunting in current case. *Orange arrow* represents other possible causes in COVID patients. Created using Microsoft Word, Washington, USA and macOs Big Sur operating system Version 11.4.

Other diagnostic tests include cardiac magnetic resonance imaging to delineate intracardiac shunts and CTA of the chest to evaluate for pulmonary AVM [1]. Closure of an atrial defect is considered in settings of increased right atrial pressure, unless the operative risk outweighs the benefit. In some instances, closure is done prophylactically. Pre-pneumonectomy is one such example [1]. Shunt fraction can be quantified over time in patients with a continued oxygen requirement by evaluating the intracardiac shunt directly with serial echocardiography, transcranial Doppler, and right heart catheterization [28-31].

Conclusions

The clinical significance of pre-existing intracardiac shunts in the presence of new parenchymal lung disease after severe COVID-19 infections has not been described. Whether clinical benefit would be obtained through closure of the intracardiac shunt in this setting is not known. The present case highlights

the multiple interrelated mechanisms of shunting in patients with COVID-related lung disease and a PFO. Eight prior cases of POS after COVID-19 pneumonia have been reported to date but none with a known PFO [7-9]. Of these cases, only 3 patients had echocardiography to rule out the presence of a PFO [7-9]. In patients with persistent positional oxygen requirements at follow-up, quantifying shunt fraction over time through multiple modalities can guide treatment decisions.

Department and Institution Where Work Was Done

Department of Internal Medicine at Eastern Virginia Medical School, Norfolk, VA, USA.

Declaration of Figures' Authenticity

All figures submitted have been created by the authors who confirm that the images are original with no duplication and have not been previously published in whole or in part.

References:

1. Agrawal A, Palkar A, Talwar A. The multiple dimensions of platypnea-orthodeoxia syndrome: A review. *Respir Med.* 2017;129:31-38
2. Akin E, Krüger U, Braun P, et al. The platypnea-orthodeoxia syndrome. *Eur Rev Med Pharmacol Sci.* 2014;18(18):2599-604
3. Gadre A, Highland KB, Mehta A. Reversible platypnea-orthodeoxia syndrome from ventilation-perfusion mismatch in interstitial lung disease: A novel etiology. *Ann Am Thorac Soc.* 2016;13(1):137-38
4. Takhar R, Biswas R, Arora A, Jain V. Platypnoea-orthodeoxia syndrome: Novel cause for a known condition. *BMJ Case Rep.* 2014;2014:bcr2013201284
5. Bellato V, Brusa S, Balazova J, et al. Platypnea-orthodeoxia syndrome in interatrial right to left shunt postpneumonectomy. *Minerva Anestesiol.* 2008;74(6):271-75
6. Bhattacharya K, Birla R, Northridge D, Zamvar V. Platypnea-orthodeoxia syndrome: A rare complication after right pneumonectomy. *Ann Thorac Surg.* 2009;88(6):2018-19
7. Tan GP, Ho S, Fan BE, et al. Reversible platypnea-orthodeoxia in COVID-19 acute respiratory distress syndrome survivors. *Respir Physiol Neurobiol.* 2020;282:103515
8. Singh K, Kadnur H, Ray A, et al. Platypnea-orthodeoxia in a patient with severe COVID-19 pneumonia. *Monaldi Arch Chest Dis.* 2020;90(4):2020.1609
9. Tham SL, Ong PL, Lee AJY, Tay MRJ. Rehabilitation of patients with platypnea-orthodeoxia syndrome in COVID-19 pneumonia: Two case reports. *J Rehabil Med Clin Commun.* 2020;3:1000044
10. Ackermann M, Verleden SE, Kuehnel M, et al. Pulmonary vascular endothelialitis, thrombosis, and angiogenesis in COVID-19. *N Engl J Med.* 2020;383(2):120-28
11. Bryce C, Grimes Z, Pujadas E, et al. Pathophysiology of SARS-CoV-2: The Mount Sinai COVID-19 autopsy experience. *Mod Pathol.* 2021;34(8):1456-67
12. Calabrese F, Pezzuto F, Fortarezza F, et al. Pulmonary pathology and COVID-19: Lessons from autopsy. The experience of European Pulmonary Pathologists. *Virchows Arch.* 2020;477(3):359-72
13. Polak SB, Van Gool IC, Cohen D, et al. A systematic review of pathological findings in COVID-19: A pathophysiological timeline and possible mechanisms of disease progression. *Mod Pathol.* 2020;33(11):2128-38
14. Kory P, Kanne JP. SARS-CoV-2 organising pneumonia: 'Has there been a widespread failure to identify and treat this prevalent condition in COVID-19?'. *BMJ Open Respir Res.* 2020;7(1):e000724
15. Ojo AS, Balogun SA, Williams OT, Ojo OS. Pulmonary fibrosis in COVID-19 survivors: Predictive factors and risk reduction strategies. *Pulm Med.* 2020;2020:6175964
16. George PM, Wells AU, Jenkins RG. Pulmonary fibrosis and COVID-19: The potential role for antifibrotic therapy. *Lancet Respir Med.* 2020;8(8):807-15
17. Gattinoni L, Chiumello D, Rossi S. COVID-19 pneumonia: ARDS or not? *Crit Care.* 2020;24(1):154
18. Bos LDJ. COVID-19-related acute respiratory distress syndrome: Not so atypical. *Am J Respir Crit Care Med.* 2020;202(4):622-24
19. Bos LDJ, Paulus F, Vlaar APJ, et al. Subphenotyping acute respiratory distress syndrome in patients with COVID-19: Consequences for ventilator management. *Ann Am Thorac Soc.* 2020;17(9):1161-63
20. Clancy CJ, Schwartz IS, Kula B, Nguyen MH. Bacterial superinfections among persons with coronavirus disease 2019: A comprehensive review of data from postmortem studies. *Open Forum Infect Dis.* 2021;8(3):ofab065
21. Dudoignon E, Caméléna F, Deniau B, et al. Bacterial pneumonia in COVID-19 critically ill patients: A case series. *Clin Infect Dis.* 2021;72(5):905-6
22. Husain MV, Rondinaud E, Humieres C, et al. Pulmonary bacterial infections in patients hospitalized for COVID-19: A retrospective observational study. *Research Square* 2021. Available at: <https://assets.researchsquare.com/files/rs-156678/v1/01f177a6-8b29-401f-862c-be4a7284593e.pdf?c=1611947975>
23. Garcia-Vidal C, Sanjuan G, Moreno-Garcia E, et al. Incidence of co-infections and superinfections in hospitalized patients with COVID-19: A retrospective cohort study. *Clin Microbiol Infect.* 2021;27(1):83-88
24. Lansbury L, Lim B, Baskaran V, Lim WS. Co-infections in people with COVID-19: A systematic review and meta-analysis. *J Infect.* 2020;81(2):266-75
25. Longo C, Ruffini L, Zanon N, et al. Platypnea-orthodeoxia after fibrotic evolution of SARS-CoV-2 interstitial pneumonia. A case report. *Acta Biomed.* 2020 [ahead of print]
26. Mekontso Dessap A, Boissier F, Leon R, et al. Prevalence and prognosis of shunting across patent foramen ovale during acute respiratory distress syndrome. *Crit Care Med.* 2010;38(9):1786-92
27. West JB. *Respiratory physiology: The essentials.* Baltimore, MD and Philadelphia, PA: Wolters Kluwer/Lippincott Williams & Wilkins, 2008
28. Mahmoud AN, Elgendy IY, Agarwal N, et al. Identification and quantification of patent foramen ovale-mediated shunts: Echocardiography and transcranial Doppler. *Interv Cardiol Clin.* 2017;6(4):495-504
29. Kumar P, Rusheen J, Tobis JM. A comparison of methods to determine patent foramen ovale size. *Catheter Cardiovasc Interv.* 2020;96(6):E621-29
30. Yang J, Zhang H, Wang Y, et al. The efficacy of contrast transthoracic echocardiography and contrast transcranial Doppler for the detection of patent foramen ovale related to cryptogenic stroke. *Biomed Res Int.* 2020;2020:1513409
31. Yang X, Wang H, Wei Y, et al. Diagnosis of patent foramen ovale: the combination of contrast transcranial Doppler, contrast transthoracic echocardiography, and contrast transesophageal echocardiography. *Biomed Res Int.* 2020;2020:8701759